Received: 17 March 2023 | Revised: 6 August 2023 | Accepted: 16 August 2023

DOI: 10.1002/bit.28537

ARTICLE

BIOTECHNOLOGY AND BIOENGINEERING WILEY

Integrated continuous downstream process of monoclonal antibody developed by converting the batch platform process based on the process characterization

Fuminori Konoike[1] | Masatoshi Taniguchi[1] | Shuichi Yamamoto[1,2]

[1]Manufacturing Technology Association of Biologics, Shin-kawa, Chuo-ku, Japan

[2]Biomedical Engineering Center (YUBEC), Graduate School of Science and Technology for Innovation, Yamaguchi University, Ube, Japan

Correspondence
Shuichi Yamamoto, Biomedical Engineering Center (YUBEC), Graduate School of Science and Technology for Innovation, Yamaguchi University, Ube 755-8611, Japan.
Email: shuichi@yamaguchi-u.ac.jp

Funding information
Japan Agency for Medical Research and Development, Grant/Award Numbers: JP18ae0101056, JP18ae0101057, JP18ae0101058, JP21ae0121016

Abstract

A continuous downstream process of monoclonal antibody was developed based on the process characterization. Periodic-counter current chromatography (PCCC) with two protein A columns was used for the capture step. For low pH virus inactivation (VI), a batch reactor was employed, which can work as a surge (buffer) tank. Flow-through chromatography (FTC) with two connected columns of different separation modes (anion-mixed mode and cation exchange) was designed as a polish step. After 24 h PCCC run, the collected pool was processed for VI. After adjusting pH and electric conductivity, the solution was fed to the two connected FTC columns for 24 h. Virus filter was also connected to the exit of the connected-column. PCCC and FTC were run in parallel. Six runs of different feed rates (0.5–10 L/day) and feed concentrations (1–3.2 g/L) were performed with protein A columns of 1–5 mL and FTC columns of 3–10 mL. The largest run (feed rate 10 L/day, feed concentration 2 g/L) was carried out at a GMP facility with 15 mL protein A columns and 100 mL FTC columns. Good recovery and purity values were obtained for all runs. The process was found to be flexible and stable for feed fluctuations. Only three surge or pool tanks were needed in addition to the final product pool tank.

KEYWORDS
buffer consumption, continuous downstream process, flow-through chromatography, monoclonal antibody, periodic counter current chromatography, productivity

1 | INTRODUCTION

As downstream process (DSP) of monoclonal antibody (mAb) includes several liquid chromatography (LC) steps, and other operations such as low pH virus inactivation (VI), it is important to consider how each batch operation is converted to a continuous or pseudo-continuous operation to develop an efficient continuous DSP (CDSP). Although many papers have been published on CDSP or intensified/integrated DSP (Chen et al., 2022; David et al., 2020; Gomis-Fons et al., 2020; Jungbauer, 2013; Karst et al., 2018; National Institute for Innovation in Manufacturing Biopharmaceuticals [NIIMBL], 2022; Ötes et al., 2017; Rathore et al., 2023; Schwarz et al., 2022; Shi et al., 2022; Shukla et al., 2017; Somasundaram et al., 2018; Vogg et al., 2018; Xu et al., 2020; Yang et al., 2019; Zydney, 2016), it is still not clear how to evaluate the benefits of CDSP properly.

We have developed an integrated CDSP (ICDSP) based on process characterization and understanding. Basically, we tried to convert a typical mAb platform DSP to ICDSP without changing each unit operation. Namely, protein A chromatography was used for the 1st capture step, followed by low pH VI. For the polish step, two chromatography columns of different separation modes were employed. Different unit operation such as precipitation was tested for continuous capture of mAb (Ferreira-Faria et al., 2023; Li et al., 2019; Royo et al., 2023). Such unit operations were not adopted in this study as commercial equipment is not available and finding suitable experimental conditions is time-consuming. For this purpose, each unit operation was characterized based on the mechanistic-model analysis. Then, we tried to find a way to connect (integrate) unit operations. We also aimed to develop ICDSP, which is easy to scale-down and scale-up (flexible process).

For the first capture step, a two-column periodic counter-current chromatography (2C-PCCC) system with protein A columns was chosen. After the capture step, a low pH VI was carried out with a batch reactor, which can work also as a surge tank. Then, the polish step was carried out by connected two LC columns of different separation modes by a flow-through chromatography (FTC) operation. A virus filter was also connected to the 2nd column of the polish step.

Our ICDSP was carried out according to the following schedule. After 24-h operation of PCCC, the recovered pool was transferred to the batch VI process, which performed 1 h incubation at an assigned low pH. The solution pH and the electric conductivity were then adjusted for the polishing FTC step. Then, the FTC step started. PCCC and FTC were operated in parallel. After each operation for 24 h, the lines of PCCC setup were cleaned, and the FTC columns and the VF were replaced.

The continuous operations for 5 days were carried out (total 7 runs) with different mAb concentrations (1–3.2 g/L), feed flow rates (0.5–10 L/day), and column volumes (1–100 mL) to confirm the process efficiency and stability. The yield and purity values were determined with the standard analytical methods to confirm that the product quality is acceptable. We also examined how to improve the process performance of ICDSP based on several evaluation indexes such as solvent consumption.

2 | MATERIALS AND METHODS

2.1 | Cell culture process

Based on a new Chinese hamster ovary (CHO)-MK cell line established at our consortium*, the CHO-MK derived antibody producing cell line was developed by Chitose Laboratory Inc., and used for the cell culture in this study (Horiuchi, 2019).

For the batch cell culture, a 50 L single-use bag (working volume 40–50 L) from ZACROS (Fujimori Kogyo Co., Ltd.) was used. The bag was mixed by shaking with a circular movement.

The continuous perfusion cell culture runs were performed either in alternating tangential flow (ATF) mode using hollow fiber membrane from Repligen with a 2L glass vessel bioreactor BCP (working volume 0.6 L) from ABLE Corporation for Run 4 in Table 2 or tangential flow filtration (TFF) mode using a hollow fiber membrane from Toray with a 10 L ZACROS single-use bag (working volume 9.4 L) for Run 7 in Table 2.

Chemically defined media prepared by FUJIFILM Wako Chemical was used both for the batch and the continuous cell cultures.

Clarified supernatant containing monoclonal IgG (mAb) from the cell culture fluid was used as the feed material for Runs 1–3, 5, and 6. Purified mAb solutions from the clarified supernatant were also used for measuring the breakthrough curves (BTCs).

2.2 | Capture chromatography process by protein A columns

The following protein A gels (resins or media) were used in this study; KanCapA 3G (KC3) (particle diameter $d_p = 75$ µm) from Kaneka Corporation and Amsphere A3 (AA3) ($d_p = 50$ µm) from JSR Corporation. OPUS MiniChrom columns packed with KC3 (0.8 cm i.d. × 2 cm, total bed volume $V_t = 1$ mL; 0.8 cm i.d. × 10 cm, $V_t = 5$ mL) supplied from Repligen were used for KC3 (V_t packed bed volume). AA3 was self-packed to Cytiva Tricorn empty columns (0.5 cm i.d. × 5 cm, $V_t = 1$ mL). For larger protein A columns, self-packed columns were used (1.6 cm i.d. × 7.5 cm, $V_t = 15$ mL).

BTCs of purified mAb solutions were measured by ÄKTA pure, ÄKTA pcc (Cytiva), and Contichrom CUBE HPLC 30 system (YMC Co., Ltd.). Experiments were carried out at different mAb concentrations and flow rates until BT% ($=C/C_F \times 100$) reached around 70% (C_F is the sample mAb concentration, and C is the concentration at the column outlet).

Twenty mM phosphate with 150 mM NaCl at pH 7.5 was used for equilibration and wash operation. One hundred mM acetic acid at pH 3.0 (Run 3, 6) and 60 mM acetic acid at pH 3.6 (Run 1, 2, 4, 5, 7) were used as elution buffer, and 0.1 M NaOH was used for CIP.

For determining the operating conditions of 2C-PCCC by Contichrom CUBE, the embedded software was used. The loading time t_L for the tandem column and the flow rate for a single column F_{F2} were calculated based on the input parameters C_F, V_t, BT% (the 1st column of the tandem column) and the non-loading protocol. F_{F1} is the flow-rate for the tandem column. The column switching was controlled by fixed time. Supporting Information: Figure S3 shows a schematic representation of 2C-PCCC flow rates (velocities). The standard nonloading protocol is shown in Table 1. The total volume needed for the nonloading period V_{NL} is 14 CV (CV: column volume).

2.3 | Low pH VI process

For low pH VI, 1 h incubation at pH 3.4 (±0.1) was chosen as the standard condition. A calibrated pH electrode (LAQUA, HORIBA) was

TABLE 1 Nonloading protocols.

	CV	RT (min)	Time (min)	
Post load wash (PLW)[a]	2	0.5	1	t_{PLW}
Wash	2	0.5	1	t_W
Elution	4	0.5	2	t_E
CIP	3	1	3	t_{CIP}
Regeneration/re-equilibration	3	1	3	t_{Reg}
Total	14	–	10	

Abbreviations: CV, column volume; RT, residence time = column bed volume/flow-rate.

[a]PLW was performed with the tandem (two-connected) column after the loading.

used for adjusting the assigned pH for a laboratory scale VI batch reactor (a 50–200 mL glass beaker) with a magnetic stirrer by introducing a 0.1 M HCl solution. After 1 h incubation, the solution pH and EC were adjusted to pH 6.5 ± 0.1 and EC = 10.7 ± 1 mS/cm, respectively by using 1 M Tris (for pH) and pure water.

A prototype fully automated large-scale device was developed, which consists of a shaker-type mixer, a single-use plastic bag (up to 500 mL), and autoclavable pH and EC sensors, tube pumps for feeding 0.1 M HCl, 1 M Tris, and water. The pH and EC sensor output signals were sent to PC, which controls the tube pump flow for adjusting the pH and the conductivity of the solution in the plastic bag. The details of this equipment made by ZACROS (Fujimori Kogyo Co., Ltd.) are shown in Supporting Information: Figures S1 and S2.

Flow reactors with open tubes were tested as a continuous VI method. Residence time distribution (RTD) curves were measured by a pulse response experiment with a standard HPLC setup using open tubes of various diameters. Although various samples were used as a sample tracer, most experiments were carried out with vitamin B12 as a tracer, which was monitored at UV 280 nm.

2.4 | Polishing chromatography process

The polish step usually includes two chromatography columns of different separation modes (orthogonal modes). The following two resins from JNC were used, an anion exchange mixed mode (AEXMM) Cellufine MAX IB (90 μm cellulose beads having salt tolerant polyamine ligands partially modified with butyl groups), and a cation exchange (CEX) Cellufine MAX DexS-HbP (90 μm cellulose beads having dextran sulfate ligands). The following self-packed columns were employed (0.67 cm i.d. × 3 cm, V_t = 1 mL; 1.46 cm i.d. × 3 cm, V_t = 5 mL; 2.6 cm i.d. × 18.8 cm, V_t = 100 mL).

We decided to use a FTC operation, as it is efficient and the flow is continuous. To eliminate the buffer exchange between two FTC operations, the same buffer solution was employed so that the two columns (MAX IB and MAX DexS-HbP) can be connected in series.

A virus filter (Planova BioEX) from Asahi Kasei Medical was also connected at the exit of the second column (MAX DexS-HbP).

The flow rate F_E was chosen so that the total volume of VI treated solution V_E can be processed by carrying out a 24 h single run.

2.5 | Analytics

2.5.1 | Host cell proteins (HCPs) concentration

CHO HCP concentrations were determined with a CHO HCP ELISA kit F550 3rd generation from Cygnus Technologies according to the manufacturer's protocol.

2.5.2 | Host cell DNA concentration

Quantitative PCR (qPCR) was performed using combination of a PrepSEQ Resiudal DNA Sample preparation kit and a resDNASEQ Quantitative CHO DNA Kit (Life Technologies) for determining host cell DNA concentrations according to the manufacturer's protocol.

2.5.3 | mAb concentration

Analytical protein A HPLC was performed on a chromatography system consisting of a MU701 UV-is detector and a PU7710 pump from GL Sciences Inc. using a silica monolith protein A column from Kyoto Monotech Co., Ltd. for determining mAb concentration in a cell culture liquid. A column was used in a bind and elute mode by using 50 mM phosphate buffer with 1000 mmol/L sodium chloride at pH 7.0 as the wash mobile phase and 100 mmol/L sodium citrate at pH 3.5 as the elution mobile phase.

UV 280 nm absorption was measured using a V750 UV-visible spectrophotometer from JASCO Corporation for determining the mAb concentration in a purified solution.

2.5.4 | mAb monomer concentration

Analytical size exclusion chromatography (SEC) was performed on a Prominence LC20 chromatography system (Shimadzu) using a TSK-Gel G3000SW$_{XL}$ column (Tosoh) and mobile phase of 100 mmol/L potassium phosphate with a 200 mmol/L sodium chloride at pH 7.0 for determining mAb monomer concentration.

3 | RESULTS

3.1 | Capture step

BTCs were obtained at RT = 1 min, 2 min and 4 min (RT = V_t/F_v residence time, where V_t is the bed volume and F_v is the volumetric flow rate). They were well fitted by the constant-pattern equation

(Chen, Konoike, et al., 2021). After examining the nonloading conditions (wash, elution, CIP, and regeneration) by batch experiments, the protocol shown in Table 1 was decided and verified by 2C-PCCC experiments for 24–48 h operations.

As our nonloading protocol is short, it is advantageous to use the small number of columns for PCCC (Baur, Angarita, Muller-Spath, & Morbidelli, 2016, Baur, Angarita, Müller-Späth, Steinebach, & Morbidelli, 2016; Chen, Konoike, et al., 2021). The productivity P_C is inversely proportional of the number of columns n_c when C_F and feed volumetric flow-rate F_F are constant (Chen, Konoike, et al., 2021; Chen, Ando, et al., 2021) for $n_c > 2$.

$$P_C = C_F F_F/(n_C V_{t,C}), \tag{1}$$

where $V_{t,C}$ is the bed volume of a single column for PCCC.

P_C cannot be defined by Equation (1) for 2C-PCCC as F_F is not constant as shown in Supporting Information: Figure S3.

The sample is applied to the tandem (connected) column at $F_F = F_{F1}$ until $t = t_L$. Then, the tandem column is washed with the buffer during t_{PLW} (postload wash), and is separated to the two columns.

While the upper column (1st column) is washed (t_w), eluted (t_E), cleaned (t_{CIP}), and regenerated (t_{Reg}), the sample is applied to the another column during $t_{L,S}$ at $F_F = F_{F2}$ (single column loading). Different flow rates such as F_{F3} and F_{F4} are employed for the non-loading period (Supporting Information: Figure S3).

Since $t_{L,S}$ is equal to t_{NL}, the average volumetric flow rate F_{Fav} for the sample loading is given by

$$F_{Fav} = (F_{F1}t_L + F_{F2}t_{NL})/(t_L + t_{PLW} + t_{NL}) = (F_{F1}t_L + F_{F2}t_{NL})/t_C, \tag{2}$$

where t_C is the cycle time for 2C-PCCC.

$$t_C = t_L + t_{PLW} + t_{NL}, \tag{3}$$

$$t_{NL} = t_W + t_E + t_{CIP} + t_{Reg}. \tag{4}$$

Therefore, P_C for 2C-PCCC is calculated by Equation (5)

$$P_C = C_F F_{Fav}/(2V_{t,C}). \tag{5}$$

Another important index for evaluating the performance of PCCC is solvent consumption S_C (Chen, Konoike, et al., 2021, Chen, Ando, et al., 2021).

$$S_C = V_{NL}/M_r = V_{NL}/(C_F F_F t_L), \tag{6}$$

where V_{NL} is the total volume used for the non-loading period. $M_r = C_F F_F t_L$ is the loaded amount per cycle.

After C_F, F_F, and $V_{t,C}$ are chosen, t_L should be decided. A longer t_L will result in a smaller S_C.

For 2C-PCCC, S_C is given by Equation (7) with F_{Fav} and t_C as $M_r = C_F F_{Fav} t_c$.

$$S_C = V_{NL}/(C_F F_{Fav} t_c). \tag{7}$$

Bed utility E^* is also employed as an evaluation index for PCCC, which is defined by Equation (8) with the static binding capacity SBC.

$$E^* = M_r/\mathrm{SBC}. \tag{8}$$

As is clear from Equation (6) and Equation (8), $(E^* \times S_C)$ is constant.

Note that since the recovered volume per cycle $V_E = F_{F3}t_E$, the concentration factor CF is given by

$$\mathrm{CF} = F_{Fav}t_C/F_{F3}t_E. \tag{9}$$

In this study, PCCC for ICDSP runs were not fully optimized. Namely, a shorter t_L than the fully optimized value was chosen to secure the safety margin (factor). Similarly, $V_{t,C}$ was larger than the fully optimized value. Many published papers (Baur, Angarita, Muller-Spath, & Morbidelli, 2016, Baur, Angarita, Müller-Späth, Steinebach, & Morbidelli, 2016, Chen et al., 2020; Chen, Konoike, et al. 2021, Kaltenbrunner et al., 2016) show that similar P_C values by the batch operation can be obtained by accepting larger S_c values. A detailed analysis on the performance of 2C-PCCC has been reported (Sun et al., 2021).

It is also important to note that although the input (feed) flow is continuous, the output flow is periodic or intermittent. The averaged output flow rate F_E is smaller than F_F and the averaged output concentration C_E becomes higher than C_F as $C_F F_F = C_E F_E$ (assuming 100% recovery). This will affect the following unit operations.

3.2 | Low pH inactivation

A simple way to perform a continuous low pH VI is to use a flow reactor with an empty tube. The RTD must be known for designing a tube flow reactor. A pulse response experiment is a standard method for determining RTD curves. As shown in Supporting Information: Figure S4, a well-known Taylor dispersion Equation (10) can describe the width of RTD curves (σ = standard deviation) for an open tube (Cottet et al., 2014; Hawe et al., 2011).

$$\sigma^2 = d_{tube}^2 t_R/(96D_m), \tag{10}$$

where d_{tube} is tube diameter, L_{tube} is tube length,). $t_R = (\pi L_{tube} d_{tube}^2/4)/F_v$ is the average retention time, F_v is the volumetric flow-rate and D_m is the molecular diffusion coefficient of the tracer sample.

It is needed to have a narrow RTD curve (small σ) to ensure an assigned incubation time, t_{inc}. According to Equation(10), the RTD curve becomes wider with increasing d_{tube}. Therefore, a longer tube is needed in scaling-up with a larger d_{tube} to ensure t_{inc} (e.g., $t_{inc} = t_R$-3σ) as shown in Supporting Information: Figure S5. Detailed studies on VI with a tubular reactor including RTD analysis were reported by Amarikwa et al. (2019), Brown et al. (2022), Gillespie et al. (2019), and Klutz et al. (2015).

Another important issue is a precise pH adjustment at the inlet of the flow reactor. This requires a mixing tank with a calibrated pH probe. The volume of such tanks cannot be smaller than 30–50 mL when the size of pH probe is considered. As mentioned in INTRODUCTION, we were willing to develop an ICDSP process, which can be easily scaled-down and scaled-up. For example, the minimum F_F for this project was 0.5 L/day. As already mentioned, after PCCC, because of the concentration factor CF by Equation (9), F_E becomes smaller. For example, when CF = 10.0, $F_E = F_F/CF = F_F/10$ = 50 mL/day. Namely, it is needed to wait 24 h to start a small-scale flow reactor.

It is also important to notice that as the flow from previous operation PCCC is not continuous but intermittent (periodic), a surge tank is needed to collect the pool.

Considering these difficulties, we decided to use a batch tank reactor for VI, which can work also as a surge (buffer tank). The batch size is defined also by this tank (batch pool tank) volume, which is determined by F_E and the duration time of PCCC (National Institute for Innovation in Manufacturing Biopharmaceuticals [NIIMBL], 2022).

One of the concerns of this batch VI operation is the quality change (or stability) of mAb in protein A PCCC elution pool after 24 h storage in the tank. The average pH of the elution pools for 7 runs was 4.4 due to buffer actions of mAb. Although a slight increase of mAb aggregates was observed, they were efficiently removed by the following polishing chromatography columns. It is likely that mAb used in this study is stable. For a mAb which is not stable, it is better to adjust pH of the PCCC elution pool before storage.

3.3 | Polish step

Although FTC is easy to use, the mobile phase compositions must be chosen carefully as the separation is usually quite sensitive to a small change in the salt concentration and/or the pH (Hasegawa et al., 2020a, 2020b). In addition, since we decided to connect the two columns of different separation modes (anion-exchange mixed mode, AEXMM and cation-exchange, CEX), finding the proper mobile phase composition is a difficult task although such operation was already reported (Ichihara et al., 2019).

Experiments showed that FTC with AEXMM was effective for removing HCPs in the range of pH 7–8 and EC = 5–15 mS/cm (Supporting Information: Figure S6). For removing aggregates by FTC with CEX a lower pH 5 and a higher EC = 20 mS/cm showed a better performance. Since the two columns were connected, pH = 6.3–6.7 and EC = 9–11 mS/cm were chosen as the mobile phase. An experiment performed at pH = 6.5 and EC = 10.7 mS/cm showed a good performance, HCP 4 ppm, aggregate 0.5% and the monomer recovery 94%. Separate experiments were carried out to determine the load amount (100–400 mg-mAb/mL-column). Although the two columns were connected to eliminate a continuous buffer change operation, in-line mixing methods may be used for the continuous buffer change (Zhang et al., 2017) when the two different mobile phases are needed. It was a single-run operation for 24 h although a multiple-run operation is possible. Our intention was to have a continuous flow from the exit of ICDSP.

The detailed analysis of the two-connected FTC column operation with VF attached to the 2nd column including viral clearance studies has been reported in Shirataki et al. (2023).

3.4 | ICDSP

Since the 1st capture and 3rd polish steps are continuous and 2nd VI step is a batch operation (Figure 1a), the developed ICDSP was carried out according to the schedule shown in Figure 1b, where the overall input and output profiles are also shown(Figure 1c). Because of the periodic output signals, the averaged flow rate for FTC processes (=F_E)

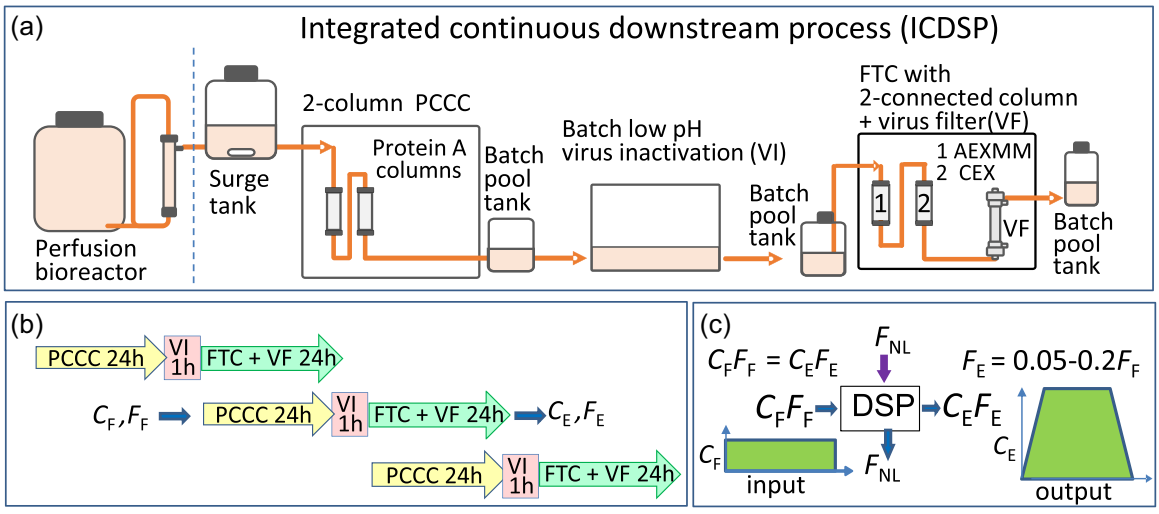

FIGURE 1 Integrated continuous downstream process (a), operation schedule (b), and flow diagram (c). C_F: feed mAb concentration, C_E: mAb concentration in the output stream, F_F: Flow rate at the inlet, F_E: Flow rate at the outlet, F_{NL}: Flow rate for the non-loading period. Because of CF by Equation (9), $F_E = F_F/CF$.

becomes lower than F_F, and C_E becomes higher than C_F as already mentioned.

The design of ICDSP is as follows.

1. $V_{t,C}$ for 2C-PCCC is determined based on C_F and F_F. Then, t_L is calculated with BT% (=30%).
2. The pool volume for 24 h V_E can be estimated with t_L as 4CV × $V_{t,C}$ × number of cycles for 24 h = 4 × $V_{t,C}$ × (24/t_C).
3. The flow rate for FTC, F_E is calculated at $F_E = V_E/24$.

2C-PCCC was run for 24 h. The collected pool was then transferred to a VI tank. The pH of the solution was adjusted to an assigned pH and left for 1 h without mixing. The pH and the EC were again adjusted for the connected FTC columns. During the VI operation, lines of 2C-PCCC were cleaned with NaOH and water. Then, the next 2C-PCCC run was started. FTC operation was also started for 24 h. 2C-PCCC and connected 2C-FTC were carried out in parallel. After 24 h operation of FTC, the columns were replaced. The virus filter was replaced as it was for a single-use system.

A batch in this CDSP is defined by the VI tank (Batch pool tank) volume and also by the duration of PCCC (24 h) (National Institute for Innovation in Manufacturing Biopharmaceuticals [NIIMBL], 2022).

We carried out 6 CDSP runs with different mAb concentrations, C_F (1–3.2 g/L), feed flow rates, F_{Fav} (0.5–3.6 L/day) and column volumes, V_t (1–10 mL) as shown in Table 2 in the laboratory. The largest scale run (Run 7) was carried out in the GMP facility with C_F = 2 g/L, F_F = 10 L/day, V_t = 15 mL for PCCC and V_t = 100 mL for FTC (see Supporting Information: Figure S7). The temperature was room temperature controlled by air conditioners (25 ± 2°C)

Run 1 was the first and the smallest scale run with the nonloading protocol shown in Supporting Information: Table S1. Then, the nonloading protocol was re-examined to reduce both time and solvent consumption. The established nonloading protocol shown in Table 1 was used for Runs 2, 3, 4, 5, and 7. For Run 6 the elution condition was slightly changed (t_E = 3.5 min, 7 CV, RT = 0.5 min).

One of the reasons of variations in P_C is due to the limited prepacked column sizes (1 and 5 mL) for the laboratory experiment (Runs 1–6). Choosing a proper column size can increase P_C.

High yield and purity were accomplished for all runs as shown in Table 3 (monomer recovery >70%, monomer purity determined by SEC > 98%, HCP concentration <10 ng/mg-IgG except for Run 3, and DNA concentration <1–4 pg/mg-IgG. We were unable to find the reason for high HCP concentrations for Run 3. The recovery of Run 7 was lower due to the misoperations (some of the pool was lost). The detailed analysis on Run 4 was published in Shirataki et al. (2023).

The continuous cell culture by the perfusion bioreactor was connected to ICDSP for Run 4 and Run 7. The feed rate and the mAb concentration varied during the continuous cell culture. The fluctuations were suppressed or diminished by the surge tank. If needed, t_L and F_{Fav} were changed at the start of PCCC 24 h run.

3.5 | Evaluation of ICDSP performance and further improvement

PCCC was already shown to be a good continuous capture method (Godawat et al., 2012). Many papers have been published on the

TABLE 2 Operating conditions and performance of integrated continuous downstream process (ICDSP) runs.

Run	C_F	F_{Fav}	t_C	$V_{t,C}$	P_C	S_c	E^*	M_r/V_t	M_{rB}/V_t	M_r/M_{rB}	$V_{t,P}$
	g/L	L/day	min	mL	$gL^{-1}h^{-1}$	L/g		mg/mL			mL
1	2	0.50	76	1[a]	20.9	0.350	0.588	52.9	47.8	1.11	3
2	1	3.56	101	5[a]	14.9	0.280	0.556	50.0	37.0	1.35	10
3	1	2.41	20	1[b]	50.1	0.419	0.464	33.4	22.0	1.52	5
4[c]	2.4	1.10	22	1[a]	55.0	0.347	0.448	40.3	28.9	1.39	3
5	3.2	3.48	31	5[a]	46.5	0.292	0.533	48.0	39.0	1.23	10
6[d]	3.1	1.25	16	1[b]	80.6	0.396	0.597	43.0	33.7	1.27	3
7[e]	2	10.61	57	15[a]	29.5	0.250	0.622	56.0	38.0	1.47	100

[a]Kaneka KanCapA 3G.
[b]JSR Amsphere A3.
[c]Connected to perfusion reactor (2L).
[d]Maximum periodic-counter current chromatography (PCCC) cycles (124).
[e]Connected to perfusion reactor (10L) at GMP facility.
$V_{t,C}$ column bed volume of 2C-PCCC.
$V_{t,P}$ column bed volume of flow-through chromatography (FTC).
S_c buffer consumption per recovered mAb for PCCC.
E^* bed utility.
M_r loaded amount of mAb for PCCC.
M_{rB} loaded amount of mAb for batch operation.

TABLE 3 Product quality of integrated continuous downstream process (ICDSP) runs.

Run	C_F	F_{Fav}	DNA	HCP	Aggregate	Monomer	Recovery
	g/L	L/day	ppb	ppm	%	%	%
1	2	0.50	1	1–3	0.7–1.3	98.7–99.3	76–83
2	1	3.56	4	2–4	1.3	98.7	78–81
3	1	2.41	1	20–35	1.3–1.8	98.2–98.7	88–91
4	2.4	1.10	1–3	0–12	0.7–0.8	99.2–99.3	72–92
5	3.2	3.48	ND	1–2	0.8–1	99.0–99.2	97–98
6	3.1	1.25	ND	1–3	0.2	99.8	81–93
7	2	10.61	<1	0–4	0.1–2.5	97.5–99.9	40–71

Note: Typical impurity concentrations of feed; HCP = 300,000 ng/mg IgG, DNA = 200,000 pg/mg-IgG; Aggregate 3%. Abbreviation: ND, not determined.

productivity P_C of PCCC defined by Equation (1) and the comparison with the values by batch operation. P_C values in Table 2 are not high compared with the literature values (Baur, Angarita, Muller-Spath, & Morbidelli, 2016, Baur, Angarita, Müller-Späth, Steinebach, & Morbidelli, 2016, Chen, Konoike, et al., 2021, Kaltenbrunner et al., 2016). High productivities can be obtained even with repeated batch (cyclic) operation (Chen et al., 2020). Low P_C values in this study are due to the rather large safety factor, and the prepacked column sizes for the laboratory runs as mentioned.

Table 2 also includes the calculated loaded amount per column volume, M_{rB} for the batch operation based on the $DBC_{10\%}$ *versus* RT data from the measured BTCs. $DBC_{10\%}$ is dynamic binding capacity (DBC) calculated from V_B at BT% = 10% (V_B: breakthrough volume). M_r/M_{rB} is one of the criteria to show the benefit of PCCC compared with the repeated batch operation. M_r/M_{rB} values for Runs 1–7 range from 1.1 to 2.0. Similar findings were reported by Chen et al. (2022) when batch DSP was converted to CDSP.

Another evaluation index S_C defined by Equation (7) becomes minimum at $M_r = SBC \times V_t$. The minimum $S_{c,\ min} = 14/SBC = 14/90 = 0.156$. As already mentioned S_C values shown in Table 2 are small (especially for Run 7) although they are not fully optimized. Figure 2 shows S_c and E^* as a function of P_C. S_C increases with P_C whereas E^* decreases with P_C. Note that $(Sc \times E^*)$ is constant as mentioned before.

The evaluation of the whole (total) CDSP performance is difficult as the productivity cannot easily be defined. Several papers are available on the cost comparison between batch and continuous processes (Arnold et al., 2019). The solvent needed for FTC process is the equilibrium buffer and the same buffer for the elution after the sample loading. Since it is a single run for 24 h and the columns were replaced after 24 h operation, the solvent consumption for ICDSP FTC operations is the same as that for the batch operation.

Our ICDSP was found to be applicable to $F_F = 0.5–10$ L/day. Since P_C can be increased up to 50–60 $gL^{-1}h^{-1}$ according to our previous paper (Chen, Konoike, et al., 2021), it is possible to use Run 7 conditions for $F_F = 20 \sim 30$ L/day. Further improvement is possible to reduce S_C by increasing the sample loading time t_L.

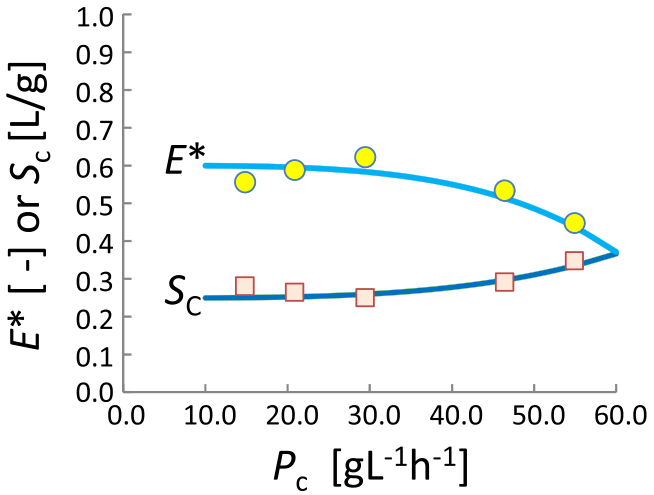

FIGURE 2 Solvent consumption S_C or bed utility E^* as a function of productivity P_C. Data for Runs 1, 2, 4, 5, and 7 are plotted. S_c for Run 1 was calculated with $V_{NL} = 14$ CV.

Our ICDSP is also flexible, and can handle fluctuations of concentrations and flow-rates as a batch VI step can work as a surge or buffer tank. Since it is not an end-to-end continuous process, the residence time for mAb production by this process depends on the duration time of PCCC. As PCCC duration time was 24 h in our 7 runs, a purified mAb can be recovered continuously after approximately 26 h (24 h PCCC, 1 h VI and 1 h FTC + VF). (According to the residence time of FTC, the purified mAb is eluted after 1 h from the start of the operation.) A shorter duration time of PCCC will reduce the total residence time of the process.

We did not employ a complicated process control procedure although several papers have been published on advanced control strategies for CDSP (Chmielowski et al., 2017; Chopda et al., 2022; Helgers et al., 2021; Rathore et al., 2021). This may contribute to a further improvement of the process performance.

Conversion of platform batch DSP to ICDSP was rather easy compared with an end-to-end CDSP, which needs a large number of

surge tanks. Three tanks were used as surge or buffer tanks in our ICDSP (Figure 1 and Supporting Information: Figure S7). Since ICDSP was converted from the (repeated) batch process, the footprint of the equipment and the column size did not change significantly. There are many other factors that can affect the adoption of CDSP (Rathore et al., 2023).

4 | CONCLUSION

An integrated continuous DSP consisting of PCCC with two protein A columns, a batch low pH VI, and FTC by two connected columns (anion-mixed mode and cation exchange) with a virus filter was developed. PCCC was run for 24 h. The collected pool was incubated at low pH for VI. After adjusting pH and EC, the solution was fed to the two connected columns for 24 h as a flow-through operation. PCCC and FTC were run in parallel. Six runs of different feed rates (0.5–10 L/day) and feed concentrations (1–3 g/L) were performed with protein A columns of 1–5 mL and FTC columns of 3–10 mL. The largest run (feed rate 10 L/day, feed concentration 2 g/L) was carried out at a GMP facility with 15 mL protein A columns and 100 mL FTC columns. Good recovery and purity values were obtained for all runs. The process was found to be flexible and stable for fluctuations in feed rate and in feed concentration. Only three surge or pool tanks were needed in addition to the final product pool tank. A further improvement of the process is possible such as higher feed rates up to 20–30 L/day with the same columns for 10 L/day.

AUTHOR CONTRIBUTIONS

Fuminori Konoike and Masatoshi Taniguchi performed experiments while they were working for Manufacturing Technology Association of Biologics (MAB) temporarily based on the discussion with Shuichi Yamamoto, and analyzed the data. Shuichi Yamamoto wrote the paper based on discussion with Fuminori Konoike and Masatoshi Taniguchi.

ACKNOWLEDGMENTS

This research was partially supported by AMED (Japan Agency for Medical Research and Development) under Grant Number JP18ae0101056, JP18ae0101057, JP18ae0101058, and JP21ae0121016.

CONFLICT OF INTEREST STATEMENT

The authors declare no conflict of interest.

DATA AVAILABILITY STATEMENT

Currently, we are not able to share our data. However, we will try to find a way to do it.

ORCID

Shuichi Yamamoto http://orcid.org/0000-0002-6756-9141

REFERENCES

Amarikwa, L., Orozco, R., Brown, M., & Coffman, J. (2019). Impact of dean vortices on the integrity testing of a continuous viral inactivation reactor. *Biotechnology Journal*, *14*, 1700726.

Arnold, L., Lee, K., Rucker-Pezzini, J., & Lee, J. H. (2019). Implementation of fully integrated continuous antibody processing: Effects on productivity and COGm. *Biotechnology Journal*, *14*, 1800061.

Baur, D., Angarita, M., Muller-Spath, T., & Morbidelli, M. (2016). Optimal model-based design of the twin-column CaptureSMB process improves capacity utilization and productivity in protein A affinity capture. *Biotechnology Journal*, *11*, 135–145.

Baur, D., Angarita, M., Müller-Späth, T., Steinebach, F., & Morbidelli, M. (2016). Comparison of batch and continuous multi-column protein A capture processes by optimal design. *Biotechnology Journal*, *11*, 920–931. https://doi.org/10.1002/biot.201500481

Brown, M., Godfrey, S., Creasy, A., Salm, J., & Fahrner, R. (2022). Continuous low pH viral inactivation: Operation and scaling strategy informs viral clearance study. *Biotechnology and Bioengineering*, *119*, 2115–2121.

Chen, C. S., Ando, K., Yoshimoto, N., & Yamamoto, S. (2021). Linear flow-velocity gradient chromatography: An efficient method for increasing the process efficiency of batch and continuous capture chromatography of proteins. *Biotechnology and Bioengineering*, *118*, 1262–1272. https://doi.org/10.1002/bit.276492021.

Chen, C.-S., Konoike, F., Yoshimoto, N., & Yamamoto, S. (2021). A regressive approach to the design of continuous capture process with multi-column chromatography for monoclonal antibodies. *Journal of Chromatography A*, *1658*, 462604. https://doi.org/10.1016/j.chroma.2021.462604

Chen, C.-S., Yoshimoto, N., & Yamamoto, S. (2020). Prediction of the performance of capture chromatography processes of proteins and its application to the repeated cyclic operation optimization. *Journal of Chemical Engineering of Japan*, *53*, 689–697. https://doi.org/10.1252/jcej.20we116

Chen, R., Chen, X.-J., Shi, C., Jiao, B., Shi, Y., Yao, B., Lin, D.-Q., Gong, W., & Hsu, S. (2022). Converting a mAb downstream process from batch to continuous using process modeling and process analytical technology. *Biotechnology Journal*, *17*):2100351. https://doi.org/10.1002/biot.202100351

Chmielowski, R. A., Mathiasson, L., Blom, H., Go, D., Ehring, H., Khan, H., Li, H., Cutler, C., Lacki, K., Tugcu, N., & Roush, D. (2017). Definition and dynamic control of a continuous chromatography process independent of cell culture titer and impurities. *Journal of Chromatography A*, *1526*, 58–69.

Chopda, V., Gyorgypal, A., Yang, O., Singh, R., Ramachandran, R., Zhang, H., Tsilomelekis, G., Chundawat, S. P. S., & Ierapetritou, M. G. (2022). Recent advances in integrated process analytical techniques, modeling, and control strategies to enable continuous biomanufacturing of monoclonal antibodies. *Journal of Chemical Technology & Biotechnology*, *97*, 2317–2335.

Cottet, H., Biron, J. P., & Martin, M. (2014). On the optimization of operating conditions for Taylor dispersion analysis of mixtures. *The Analyst*, *139*(14), 3552–3562.

David, L., Schwan, P., Lobedann, M., Borchert, S.-O., Budde, B., Temming, M., Kuerschner, M., Alberti Aguilo, F. M., Baumarth, K., Thüte, T., Maiser, B., Blank, A., Kistler, V., Weber, N., Brandt, H., Poggel, M., Kaiser, K., Geisen, K., Oehme, F., & Schembecker, G. (2020). Side-by-side comparability of batch and continuous downstream for the production of monoclonal antibodies. *Biotechnology and Bioengineering*, *117*, 1024–1036. https://doi.org/10.1002/bit.27267

Ferreira-Faria, D., Domingos-Moreira, F., Aires-Barros, M. R., Ferreira, A., & Azevedo, A. M. (2023). Continuous precipitation of antibodies using oscillatory flow reactor: A proof of concept. *Separation and Purification Technology*, *317*, 123924.

Gillespie, C., Holstein, M., Mullin, L., Cotoni, K., Tuccelli, R., Caulmare, J., & Greenhalgh, P. (2019). Continuous in-line virus inactivation for next generation bioprocessing. *Biotechnology Journal*, *14*, 1700718.

Godawat, R., Brower, K., Jain, S., Konstantinov, K., Riske, F., & Warikoo, V. (2012). Periodic counter-current chromatography - design and operational considerations for integrated and continuous purification of proteins. *Biotechnology Journal*, *7*, 1496–1508.

Gomis-Fons, J., Schwarz, H., Zhang, L., Andersson, N., Nilsson, B., Castan, A., Solbrand, A., Stevenson, J., & Chotteau, V. (2020). Model-based design and control of a small-scale integrated continuous end-to-end mAb platform. *Biotechnology Progress*, *36*, e2995.

Hasegawa, S., Chen, C.-S., Yoshimoto, N., & Yamamoto, S. (2020a). Accelerated method for designing flow-through chromatography of proteins. *Journal of Chemical Engineering of Japan*, *53*, 206–213.

Hasegawa, S., Chen, C.-S., Yoshimoto, N., & Yamamoto, S. (2020b). Optimization of flow-through chromatography of proteins. *Journal of Chemical Engineering of Japan*, *53*, 214–221.

Hawe, A., Hulse, W. L., Jiskoot, W., & Forbes, R. T. (2011). Taylor dispersion analysis compared to dynamic light scattering for the size analysis of therapeutic peptides and proteins and their aggregates. *Pharmaceutical Research*, *28*, 2302–2310.

Helgers, H., Schmidt, A., Lohmann, L. J., Vetter, F. L., Juckers, A., Jensch, C., Mouellef, M., Zobel-Roos, S., & Strube, J. (2021). Towards autonomous operation by advanced process control process analytical technology for continuous biologics antibody manufacturing. *Processes*, *9*, 172.

Horiuchi, A. (2019). Establishment of a novel cho cell line and its application to the production of protein-based pharmaceuticals (In Japanese). *Seibutsu-kogaku Kaishi*, *97*, 328–330.

Ichihara, T., Ito, T., & Gillespie, C. (2019). Polishing approach with fully connected flow-through purification for therapeutic monoclonal antibody. *Engineering in Life Sciences*, *19*, 31–36. https://doi.org/10.1002/elsc.201800123

Jungbauer, A. (2013). Continuous downstream processing of biopharmaceuticals. *Trends in Biotechnology*, *31*, 479–492.

Kaltenbrunner, O., Diaz, L., Hu, X., & Shearer, M. (2016). Continuous bind and elute protein A capture chromatography: Optimization under process scale column constraints and comparison to batch operation. *Biotechnology Progress*, *32*, 938–948.

Karst, D. J., Steinebach, F., & Morbidelli, M. (2018). Continuous integrated manufacturing of therapeutic proteins. *Current Opinion in Biotechnology*, *53*, 76–84. https://doi.org/10.1016/j.copbio.2017.12.015

Klutz, S., Kurt, S. K., Lobedann, M., & Kockmann, N. (2015). Narrow residence time distribution in tubular reactor concept for Reynolds number range 10–100. *Chemical Engineering Research and Design*, *95*, 22–33.

Li, Z., Gu, Q., Coffman, J. L., Przybycien, T., & Zydney, A. L. (2019). Continuous precipitation for monoclonal antibody capture using countercurrent washing by microfiltration. *Biotechnology Progress*, *35*(6), e2886.

National Institute for Innovation in Manufacturing Biopharmaceuticals (NIIMBL). (2022). N-mAb: A case study to support development and adoption of integrated continuous bioprocesses for monoclonal antibodies. https://niimbl.force.com/s/n-mab

Ötes, O., Flato, H., Winderl, J., Hubbuch, J., & Capito, F. (2017). Feasibility of using continuous chromatography in downstream processing: Comparison of costs and product quality for a hybrid process vs. a conventional batch process. *Journal of Biotechnology*, *259*, 213–220.

Pons Royo, M. C., De Santis, T., Komuczki, D., Satzer, P., & Jungbauer, A. (2023). Continuous precipitation of antibodies by feeding of solid polyethylene glycol. *Separation and Purification Technology*, *304*, 122373.

Rathore, A. S., Nikita, S., Thakur, G., & Deore, N. (2021). Challenges in process control for continuous processing for production of monoclonal antibody products. *Current Opinion in Chemical Engineering*, *31*, 100671.

Rathore, A. S., Thakur, G., & Kateja, N. (2023). Continuous integrated manufacturing for biopharmaceuticals: A new paradigm or an empty promise? *Biotechnology and Bioengineering*, *120*, 333–351.

Schwarz, H., Gomis-Fons, J., Isaksson, M., Scheffel, J., Andersson, N., Andersson, A., Castan, A., Solbrand, A., Hober, S., Nilsson, B., & Chotteau, V. (2022). Integrated continuous biomanufacturing on pilot scale for acid-sensitive monoclonal antibodies. *Biotechnology and Bioengineering*, *119*, 2152–2166. https://doi.org/10.1002/bit.28120

Shi, C., Chen, X.-J., Jiao, B., Liu, P., Jing, S.-Y., Zhong, X.-Z., Chen, R., Gong, W., & Lin, D.-Q. (2022). Model-assisted process design for better evaluation and scaling up of continuous downstream bioprocessing. *Journal of Chromatography A*, *1683*, 463532. https://doi.org/10.1016/j.chroma.2022.463532

Shirataki, H., Matsumoto, Y., Konoike, F., & Yamamoto, S. (2023). Viral clearance in end-to-end integrated continuous process for mAb purification: Total flow-through integrated polishing on two columns connected to virus filtration. *Biotechnology and Bioengineering*. https://doi.org/10.1002/bit.28464

Shukla, A. A., Wolfe, L. S., Mostafa, S. S., & Norman, C. (2017). Evolving trends in mAb production processes. *Bioengineering & Translational Medicine*, *2*, 58–69. https://doi.org/10.1002/btm2.10061

Somasundaram, B., Pleitt, K., Shave, E., Baker, K., & Lua, L. H. L. (2018). Progression of continuous downstream processing of monoclonal antibodies: Current trends and challenges. *Biotechnology and Bioengineering*, *115*, 2893–2907. https://doi.org/10.1002/bit.26812

Sun, Y. N., Shi, C., Zhang, Q. L., Slater, N. K. H., Jungbauer, A., Yao, S. J., & Lin, D. Q. (2021). Comparison of protein A affinity resins for twin-column continuous capture processes: Process performance and resin characteristics. *Journal of Chromatography A*, *1654*, 462454.

Vogg, S., Müller-Späth, T., & Morbidelli, M. (2018). Current status and future challenges in continuous biochromatography. *Current Opinion in Chemical Engineering*, *22*, 138–144.

Xu, J., Xu, X., Huang, C., Angelo, J., Oliveira, C. L., Xu, M., Xu, X., Temel, D., Ding, J., Ghose, S., Borys, M. C., & Li, Z. J. (2020). Biomanufacturing evolution from conventional to intensified processes for productivity improvement: A case study. *mAbs*, *12*, 1770669. https://doi.org/10.1080/19420862.2020.1770669

Yang, O., Prabhu, S., & Ierapetritou, M. (2019). Comparison between batch and continuous monoclonal antibody production and economic analysis. *Industrial & Engineering Chemistry Research*, *58*(15), 5851–5863.

Zhang, J., Conley, L., Pieracci, J., & Ghose, S. (2017). Pool-less processing to streamline downstream purification of monoclonal antibodies. *Engineering in Life Sciences*, *17*, 117–124.

Zydney, A. L. (2016). Continuous downstream processing for high value biological products: A review. *Biotechnology and Bioengineering*, *113*, 465–475.

SUPPORTING INFORMATION

Additional supporting information can be found online in the Supporting Information section at the end of this article.

How to cite this article: Konoike, F., Taniguchi, M., & Yamamoto, S. (2024). Integrated continuous downstream process of monoclonal antibody developed by converting the batch platform process based on the process characterization. *Biotechnology and Bioengineering*, *121*, 2269–2277. https://doi.org/10.1002/bit.28537